

Simple model of membrane proteins including solvent

D. L. Pagan,^{a)} A. Shirayev, T. P. Connor, and J. D. Gunton
Department of Physics, Lehigh University, Bethlehem, Pennsylvania 18015

(Received 27 October 2005; accepted 16 March 2006; published online 9 May 2006)

We report a numerical simulation for the phase diagram of a simple two-dimensional model, similar to the one proposed by Noro and Frenkel [J. Chem. Phys. **114**, 2477 (2001)] for membrane proteins, but one that includes the role of the solvent. We first use Gibbs ensemble Monte Carlo simulations to determine the phase behavior of particles interacting via a square-well potential in two dimensions for various values of the interaction range. A phenomenological model for the solute-solvent interactions is then studied to understand how the fluid-fluid coexistence curve is modified by solute-solvent interactions. It is shown that such a model can yield systems with liquid-liquid phase separation curves that have both upper and lower critical points, as well as closed loop phase diagrams, as is the case with the corresponding three-dimensional model. © 2006 American Institute of Physics. [DOI: [10.1063/1.2193511](https://doi.org/10.1063/1.2193511)]

I. INTRODUCTION

Although there exists no theoretical framework concerning how to optimally grow protein crystals, experimentalists have produced a large number of globular protein crystals suitable for x-ray diffraction. This is evidenced by the large number of crystal structures available in the protein data bank.¹ The situation, however, is rather different for the case of membrane proteins, a class of important proteins which are characterized as being attached to a lipid membrane.² These proteins have a number of important functions, including the catalysis of specific transport of metabolites and ions across membrane barriers, the conversion of sunlight energy into chemical and electrical energies, and the reception and transduction of signals (such as neurotransmitters or hormones) across the cell membrane.³ By comparison, far fewer membrane protein structures are known than for globular proteins, due to the difficulty in crystallizing membrane proteins. Membrane proteins are embedded in the electrically insulating lipid bilayers of biological membranes. The parts of the protein surface which are in contact with the alkane chains of the lipids are highly hydrophobic, whereas their surfaces that are exposed to the aqueous media on each side of the membrane are hydrophilic. This amphiphilic nature of membrane proteins makes it difficult to crystallize them, since there are large hydrophobic and hydrophilic surface areas. As a consequence they are not soluble in aqueous solutions (unlike globular proteins), so that detergents are commonly used to isolate and purify them. The detergents are themselves amphiphilic molecules which form micelles at sufficiently large concentrations. The detergent micelles incorporate the proteins in the solubilization process. The membrane protein in the detergent micelle is then the initial material used for purification and crystallization. It has been shown that membrane proteins can often be more easily crystallized if they are forced to interact in a quasi-two-dimensional space.^{3,4} Many approaches to crystallizing

membrane proteins utilize this procedure. Thus it is of interest to know the general features of the phase behavior of quasi-two-dimensional proteins and to compare these with those for globular proteins. This is obviously a challenging problem due to the additional role of the detergent and solvent in mediating the interactions between membrane proteins.

The phase behavior of globular proteins has often been modeled using ideas from a similar problem in colloidal science. It has been shown⁵⁻¹³ that to a reasonable first approximation these proteins can be modeled using a short-range attractive interaction and a hard-core repulsion. Indirect evidence suggests that membrane proteins also interact via a short-range interaction as well. As a consequence, a generic phase diagram for membrane proteins has been proposed¹⁴ based on a short-range interaction model. In addition, a similar approach¹⁵ has been used to successfully model the phase behavior of the protein Annexin V. However, an important effect that has been largely ignored until recently is the role of the solute-solvent interactions on such phase diagrams. For three-dimensional globular proteins, crystals are grown using a combination of a variety of precipitating agents, including salts and polyethylene glycol. These agents (along with other additives to control such parameters as the pH) are used to fine-tune the interactions between proteins and control the range and strength of interactions between protein particles. Precipitating agents are also important in crystallizing membrane proteins. As a first step toward understanding the role of solute-solvent interactions in protein crystallization, a model was proposed recently¹⁶ for globular proteins interacting via a short-range potential interacting in three dimensions. In that study, it was shown that a variety of phase diagrams could be obtained for different choices of the solute-solvent parameters. In this paper we extend that study to model particles interacting in a quasi-two-dimensional plane in the presence of a solvent. We first consider the particular case of particles interacting via a square-well potential, in the absence of solvent, determining the fluid-fluid

^{a)}Electronic mail: dlpa2@lehigh.edu

coexistence curves for several different interaction ranges, using standard Monte Carlo methods. We then obtain the phase diagram for such a system taking into account solute-solvent interactions and show that there are several possible types of phase diagrams, depending on the choice of interaction parameters. Namely, the model can have an upper critical point, a lower critical point, or closed loop phase diagrams, depending on the solute-solvent interactions. Our work is an extension of the original work of Noro and Frenkel¹⁴ in that we include these solute-solvent interactions (in a very simple way).

II. COMPUTATIONAL AND THEORETICAL DETAILS

We use a square-well potential to model the attractive interactions between protein particles interacting in a two-dimensional (2D) plane. The square-well potential is given by

$$V(r) = \begin{cases} \infty, & r < \sigma \\ -\epsilon, & \sigma \leq r < \lambda\sigma \\ 0, & r \geq \lambda\sigma, \end{cases} \quad (1)$$

where the particle diameter, σ , and the well depth, ϵ , set the length and energy scale, respectively, and λ is the interaction range. We attempt to obtain the fluid-fluid coexistence curve of particles interacting in a 2D plane via Eq. (1) for the ranges $1.25 \leq \lambda \leq 2.0$. To calculate the fluid-fluid coexistence curves, we employ the Gibbs ensemble Monte Carlo method.¹⁷ This method is well suited to studying such systems away from the critical point and is a standard technique.

As noted in the Introduction, membrane proteins are often crystallized in two dimensions (2D) where, as in three dimensions (3D), various solvents are used to promote crystallization. These precipitating agents thus play an important part in the crystallization process. As noted in the Introduction, a simple phenomenological model for the role of solvent has been proposed.¹⁶ The multicomponent system (i.e., proteins plus solvent) is modeled as a binary system in which the solute particle is much bigger than the solvent. It is also assumed that the effects of the other components are subsumed in the effective solute-solvent interaction.

The total energy of a protein system interacting via a short-range potential can be written as

$$U_0(\mathbf{r}^N) = \frac{1}{2} \sum_{i \neq j} U_0(|\mathbf{r}_i - \mathbf{r}_j|), \quad (2)$$

where the subscript “0” denotes the potential of the protein in the absence of solvent. The model that incorporates the effect of solvent has a total potential

$$U = U_0 + \sum (\epsilon_w - k_B T \Delta s_w) n_w^{(i)}(\mathbf{r}^N), \quad (3)$$

where $n_w^{(i)}$ is the number of water molecules around the i th particle and ϵ_w and s_w are the interaction energies and entropy of the solvent, respectively. The authors show¹⁶ that this solute-solvent interaction leads to an effective protein-protein square-well interaction whose strength is given by $\tilde{\epsilon} = \epsilon + 2\epsilon_w - 2k_B T \Delta s_w$. Thus, the Boltzmann weighting factor for the system with solvent is the same as the one without

solvent, except that $\tilde{\epsilon}$ replaces ϵ . This yields several results for the model with solvent in terms of the behavior of the model without solvent. For example, the phase diagram for the system with solute-solvent interactions is given by

$$k_B T_{\text{coex}} = \frac{(\epsilon_0 + 2\epsilon_w)}{1 + 2\Delta s_w} \tau(\rho), \quad (4)$$

where $\tau(\rho)$ is the functional form of the coexistence curve (denoting two coexisting phases) without solvent. This expression is independent of dimensionality. Similarly, the radial distribution function for the system with solute-solvent interactions is given in terms of such interactions by

$$g_s(r) \equiv g_0(r; \tilde{\epsilon}). \quad (5)$$

Correspondingly, the structure factor for the system with solute-solvent interactions is given by

$$S_s(q) = S_0(q; \tilde{\epsilon}). \quad (6)$$

For a complete discussion of the model, the reader is referred to Ref. 16.

We obtain the fluid-fluid coexistence curves of $N=250$ particles without solvent via Gibbs ensemble¹⁷ Monte Carlo simulations. We then use Eq. (4) to determine the coexistence curves of the particles interacting via Eq. (1) that includes the solute-solvent interactions. Equilibration runs lasted 10×10^6 Monte Carlo (MC) steps, whereas production runs lasted 20×10^6 MC steps. Simulations were initialized from a liquid configuration.

Isobaric-isothermal (NPT) Monte Carlo simulations¹⁸ were employed to sample the fluid and solid phases of the 2D system without solvent. For sufficiently low ranges of λ , we observed a tendency for the fluid to crystallize and the solid phase to melt at appropriate pressures, as found in another study.¹⁴ To overcome this difficulty, we employ a biasing parameter which allows us to force the system into either a liquid or solid state. We use the bond-order parameter¹⁹ defined by

$$Q_{lm} \equiv Y_{lm}(\phi(\mathbf{r})), \quad (7)$$

where Y_{lm} are the spherical harmonics. We calculate the bond-order parameter,¹⁹ Q_6 , which has a nonzero value for a two-dimensional solid and a zero value for the liquid. Q_6 is calculated¹⁹ as

$$Q_l = \left[\frac{4\pi}{2l+1} \sum_{m=-l}^{m=l} \langle Q_{lm} \rangle^2 \right]^{1/2}. \quad (8)$$

Less than 5% of all configurations are rejected in any simulation of the liquid or solid. Using this order parameter we are able to sample fluid and solid phases and measure the radial distribution function, $g(r)$, and the bond-order correlation function, $g_6(r)$, given by

$$g_6(r) = \langle \psi_6^*(\mathbf{r}_j) \psi_6(\mathbf{r}_i) \rangle, \quad (9)$$

where the local bond-order parameter $\psi(\mathbf{r}_i)$ for particle i at position \mathbf{r}_i is given by

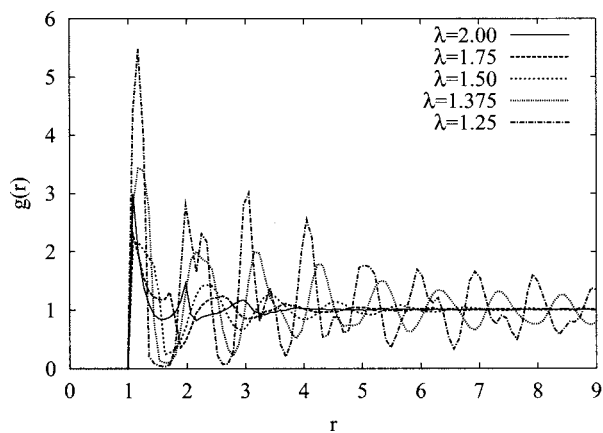


FIG. 1. Radial distribution functions for the ranges $1.25 \leq \lambda \leq 2.0$. Long-range order begins to appear for ranges where $\lambda \leq 1.375$.

$$\psi_6(\mathbf{r}_i) = \frac{\sum_k w(r_{ik}) \exp(i6\theta_{ik})}{\sum_k w(r_{ik})}. \quad (10)$$

The summation is over neighboring particles k of particle i ; θ_{ik} is the angle between the vector $(\mathbf{r}_i - \mathbf{r}_k)$ and a fixed reference axis. The weighting factor w is used to define nearest neighbors.

III. RESULTS AND DISCUSSION

The fluid-fluid coexistence curves have been calculated using Gibbs ensemble Monte Carlo. Below $\lambda = 1.50$, we were unable to obtain a fluid-fluid coexistence curve. For particles interacting via a range of attraction of $\lambda = 1.375$, we observe that the expected fluid branch of the coexistence curve tends to solidify, exhibiting a structure consistent with a solid. This was observed for the range $\lambda = 1.25$ as well. For $\lambda = 1.50$ and above, however, we do indeed observe fluid-fluid coexistence. This was verified by calculating both the radial distribution function, $g(r)$, and the bond-order correlation function, $g_6(r)$, calculated as described previously. Figures 1 and 2 show this behavior for the various ranges considered. Similar behavior has been observed for another system of particles interacting via a short-range potential¹⁴ in 2D. In that study, this phenomenon was observed at short ranges of at-

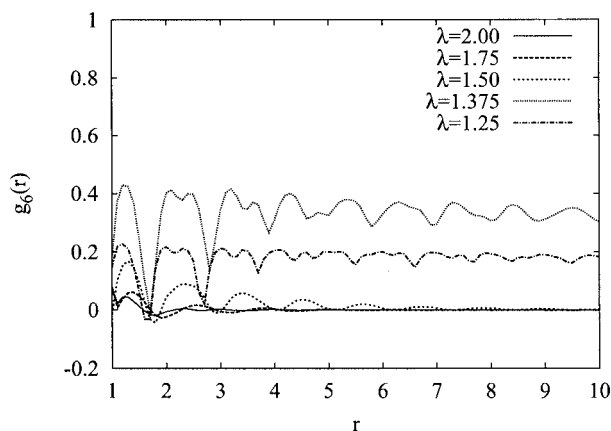


FIG. 2. Bond-order correlation functions for the ranges $1.25 \leq \lambda \leq 2.0$. A structure consistent with a solid is found for ranges where $\lambda \leq 1.375$.

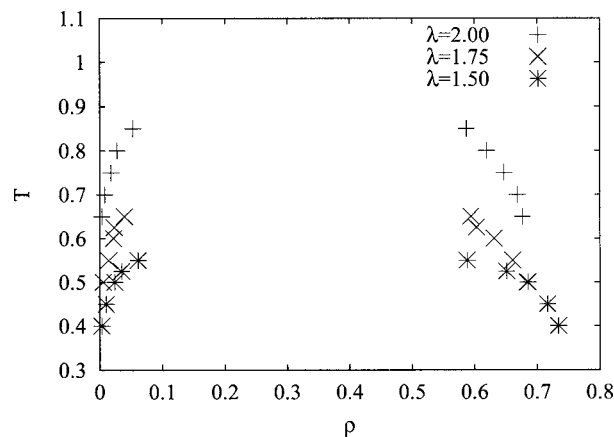


FIG. 3. Fluid-fluid coexistence curves for the ranges $\lambda = 2.0, 1.75$, and 1.50 for the 2D square-well model.

traction corresponding to the case where the spinodal curve is metastable with respect to the liquidus-solidus curve, suggesting that the binodal curve is metastable as well. It has been proposed¹⁴ that the free-energy barrier to be overcome is much smaller in 2D than in 3D. Thus, at sufficiently low ranges of interaction, the metastable fluid-fluid coexistence curve cannot be sampled.

The fluid-fluid coexistence curves for values $\lambda \geq 1.50$ are shown in Fig. 3. It is worthwhile to compare these coexistence curves to their 3D counterparts.²⁰ The critical temperatures in 2D at these interaction ranges, λ , are relatively close to each other as compared to those in 3D. Also, the critical temperatures are lower than those in 3D. The critical densities are different as well, yet they exhibit the same behavior as their 3D counterparts—the critical density increases with decreasing λ .

To obtain the fluid-fluid coexistence curves with solvent we use Eq. (4). It has been shown¹⁶ that for appropriate choices of the parameters ϵ_w and s_w , a variety of phase diagrams can be realized. We choose the parameters $\epsilon_w = -1.0$ and $s_w = -1.50$ to see how the 2D fluid-fluid coexistence curves are affected in the presence of solvent with these particular interaction parameters. For these values of the parameters, it has been shown¹⁶ for the 3D square-well model that the phase diagram at $\lambda = 1.25$ has a lower critical point,

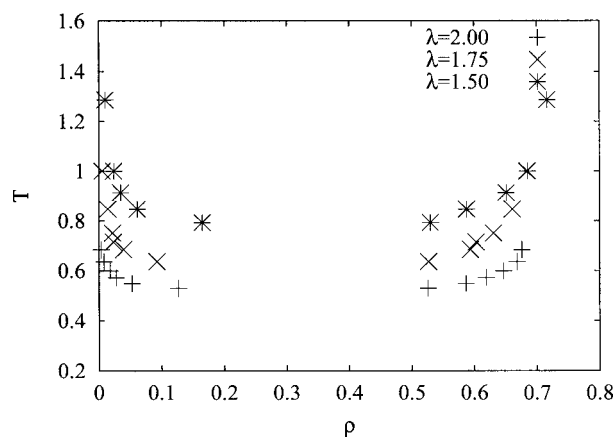


FIG. 4. Fluid-fluid coexistence curves for the ranges $\lambda = 2.0, 1.75$, and 1.50 for the 2D square-well model in the presence of the solvent.

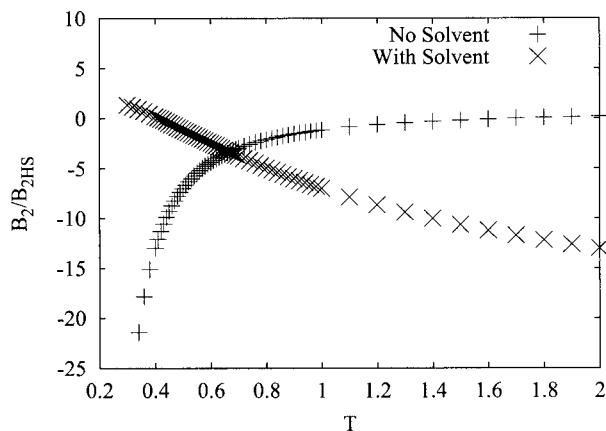


FIG. 5. Second virial coefficient as a function of temperature both in the absence and presence of the solvent.

whereas the model in the absence of solute-solvent interaction has an upper critical point. We find a similar behavior in 2D. It remains to be seen, however, if whether membrane proteins (or colloids) constrained to interact in quasi-two-dimensional space exhibit such phase diagrams. Figure 4 shows the fluid-fluid coexistence curves at the ranges we have studied, with solvent.

As discussed previously, many agents are added to a protein-solvent mixture to control the protein-protein interaction range. The second virial coefficient B_2 , is a measure of the net interaction and is commonly used as a means of determining the window for optimal globular protein crystallization.²¹ This is presumably also true for membrane proteins. Therefore we show B_2/B_2^{HS} as a function of temperature in Fig. 5. (B_2^{HS} is the second virial coefficient of hard spheres.) In the absence of solute-solvent interactions, $B_2 \rightarrow B_2^{\text{HS}}$ as $T \rightarrow \infty$, as the hard sphere interaction dominates. However, in the presence of solute-solvent interactions $B_2 \rightarrow B_2^{\text{HS}}$ as $T \rightarrow \frac{1}{3}$. This occurs because the effective interaction between particles, $\tilde{\epsilon}$, vanishes at that temperature, leaving only the hard sphere interaction. (The same situation occurs in three dimensions.) Although the second virial coefficient is only a function of temperature, if one plots its behavior along the coexistence curve, it becomes a function of density through the dependence of the coexistence tem-

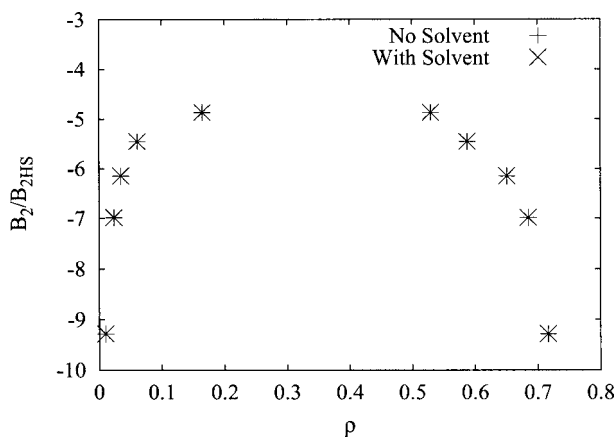


FIG. 6. Second virial coefficient as a function of density both in the absence and presence of the solvent.

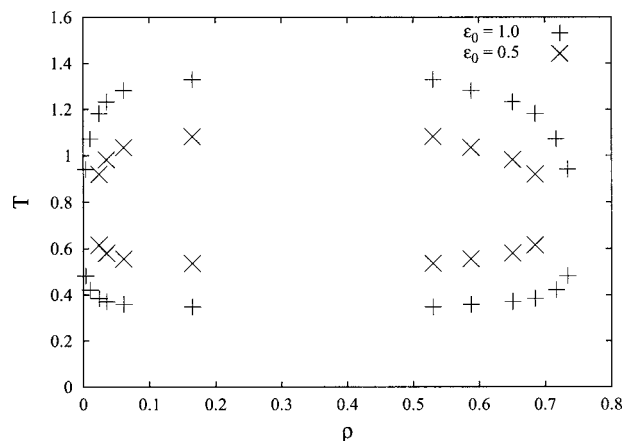


FIG. 7. Fluid-fluid coexistence curves for the two-dimensional square-well model with solvent. The closed loop behavior is obtained using a simple model to illustrate the effects of temperature-dependent parameters in the model on the fluid-fluid coexistence curve, as discussed in the text.

perature on density. We show this dependence in Fig. 6. Along such a path the second virial coefficients with and without solute-solvent interaction are equal.

The model studied here can be also used to study the case in which the effective interactions introduced by the solute-solvent interaction are temperature dependent. This can be obtained from Eq. (4) by introducing temperature-dependent parameters and ϵ_w and Δs_w . To illustrate this situation, we use the four-level model of Muller, Lee, and Graziano²²⁻²⁴ (MLG) for water, as it provides a simple example of such temperature-dependent parameters. (We are not claiming that such a model is realistic in our case, but it does provide us with an illustrative example.) It can be shown¹⁶ that ϵ_w and Δs_w can be obtained in the MLG model as $\epsilon_w(kT) = E_s - E_b$ and $\Delta s_w(kT) = S_s - S_b$ where the former and latter equations are the differences in energy and entropy in the bulk and shell states, respectively. (See Ref. 24 for the definition of these energies and entropies.) Figure 7 shows closed loop fluid-fluid coexistence curves for choices of the parameter $\epsilon_0 = 0.5$ and $\epsilon_0 = 1.0$ in Eq. (4).

Finally, we briefly discuss the possibility of a hexatic phase for our model. To test for this possibility, we determine the radial distribution function $g(r)$ and the bond-order cor-

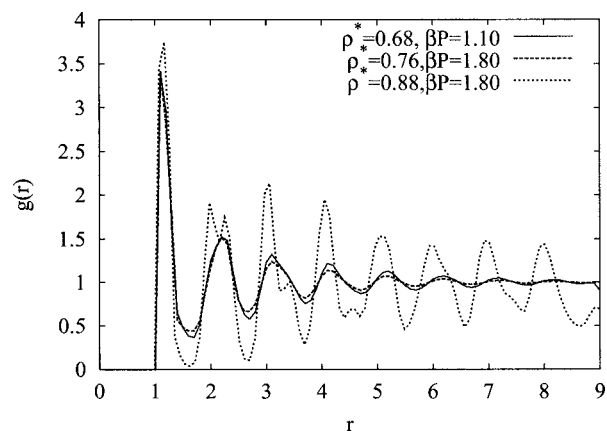


FIG. 8. Typical radial distribution functions for the liquid and solid phases at various densities ρ and pressure βP .

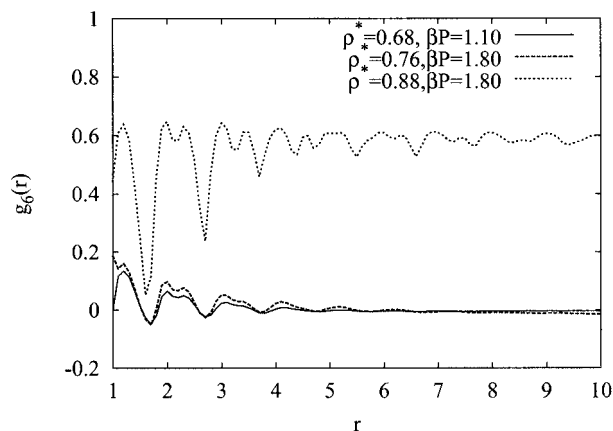


FIG. 9. Typical bond-order correlation functions for the liquid and solid phases at various densities ρ and pressures βP .

relation function $g_6(r)$ for the fluid and solid phases at $\lambda=1.25$. Figures 8 and 9 show our results for typical values of pressure and temperature in the liquid and solid phases. Figure 8 shows two typical $g(r)$ plots corresponding to a fluid phase as well as one corresponding to a solid phase. Figure 9 shows our calculation of $g_6(r)$. For a hexatic phase, one would expect an algebraic decay. Our plot shows behavior typical of fluids and solids; $g_6(r)$ decays rapidly to zero in the fluid phase, indicating absence of long-range order, while that of the solid decays to a constant value. We see no evidence of a hexatic phase for our two-dimensional model. However, because our system is quite small, finite size effects could be important. Therefore our results are certainly not definitive.

IV. CONCLUSION

We have studied the phase behavior of a simple model that is meant to describe the generic features of membrane proteins confined to a quasi-two-dimensional geometry. In particular, we have shown that a simple phenomenological model for the solute-solvent interactions can yield phase dia-

grams with upper and lower fluid-fluid critical points, as well as closed loops, depending on the choice of interaction parameters.

ACKNOWLEDGMENTS

This work was supported by the G. Harold Mathers and Leila Y. Mathers Foundation and by the National Science Foundation, Grant No. DMR-0302598.

- ¹H. M. Berman, J. Westbrook, Z. Feng, G. Gilliland, T. N. Bhat, H. Weissig, I. N. Shindyalov, and P. E. Bourne, *Nucleic Acids Res.* **28**, 235 (2000).
- ²S. J. Singer and G. L. Nicolson, *Science* **175**, 720 (1972).
- ³H. Michel, *Trends Biochem. Sci.* **8**, 56 (1983).
- ⁴J.-L. Rigaud, M. Chami, O. Lambert, D. Levy, and J.-L. Ranck, *Biochim. Biophys. Acta* **1508**, 112 (2000).
- ⁵A. P. Gast, C. K. Hall, and W. B. Russel, *J. Colloid Interface Sci.* **96**, 251 (1983).
- ⁶H. N. W. Lekkerkerker, W. C-K. Poon, P. N. Pusey, A. Stroobants, and P. B. Warren, *Europhys. Lett.* **20**, 559 (1992); C. F. Tejero, A. Daanoun, H. N. W. Lekkerkerker, and M. Baus, *Phys. Rev. Lett.* **73**, 752 (1994).
- ⁷M. H. J. Hagen and D. Frenkel, *J. Chem. Phys.* **101**, 4093 (1994).
- ⁸D. Rosenbaum, P. C. Zamora, and C. F. Zukoski, *Phys. Rev. Lett.* **76**, 150 (1996).
- ⁹P. R. ten Wolde and D. Frenkel, *Science* **277**, 1975 (1997).
- ¹⁰D. W. Oxtoby and V. Talanquer, *J. Chem. Phys.* **101**, 223 (1998).
- ¹¹D. L. Pagan, M. E. Gracheva, and J. D. Gunton, *J. Chem. Phys.* **120**, 8292 (2004).
- ¹²A. Shiryayev and J. D. Gunton, *J. Chem. Phys.* **120**, 8398 (2004).
- ¹³D. L. Pagan and J. D. Gunton, *J. Chem. Phys.* **122**, 184515 (2005).
- ¹⁴M. G. Noro and D. Frenkel, *J. Chem. Phys.* **114**, 2477 (2001).
- ¹⁵M. A. Bates, M. G. Noro, and D. Frenkel, *J. Chem. Phys.* **116**, 7217 (2002).
- ¹⁶A. Shiryayev, D. L. Pagan, J. D. Gunton, D. Rhen, A. Saxena, and T. Lookman, *J. Chem. Phys.* **122**, 234911 (2005).
- ¹⁷A. Z. Panagiotopoulos, *Mol. Phys.* **61**, 813 (1987).
- ¹⁸D. Frenkel and B. Smit, *Understanding Molecular Simulation* (Academic, San Diego, 2002).
- ¹⁹P. J. Steinhardt, D. R. Nelson, and M. Ronchetti, *Phys. Rev. B* **28**, 784 (1983).
- ²⁰L. Vega, E. de Miguel, L. F. Rull, G. Jackson, and I. A. McLure, *J. Chem. Phys.* **96**, 2296 (1992).
- ²¹A. George and W. Wilson, *Annu. Rev. Biophys. Bioeng.* **50**, 361 (1994).
- ²²N. Muller, *Acc. Chem. Res.* **23**, 23 (1990).
- ²³B. Lee and G. Graziano, *J. Am. Chem. Soc.* **118**, 5163 (1996).
- ²⁴S. Moelbert and P. D. L. Rios, *Macromolecules* **36**, 5845 (2003).